LEVEL II

12

TECHNICAL REPORT ARBRL-TR-02335

(Supersedes IMR No. 696)

A SIMPLE METHOD FOR PREDICTING MUZZLE BRAKE EFFECTIVENESS AND BAFFLE-SURFACE PRESSURE

Kevin S. Fansler

Jun[redacted]981

37

Final rept.

US ARMY ARMAMENT RESEARCH AND DEVELOPMENT COMMAND
BALLISTIC RESEARCH LABORATORY
ABERDEEN PROVING GROUND, MARYLAND

1L161102 AH43

Approved for public release; distribution unlimited.

393171

UNCLASSIFIED

SECURITY CLASSIFICATION OF THIS PAGE (When Data Entered)

REPORT DOCUMENTAT' ,N PAGE		READ INSTRUCTIONS BEFORE COMPLETING FORM
1. REPORT NUMBER TECHNICAL REPORT ARBRL-TR-02335	2. GOVT ACCESSION NO. AD-A102 349	3 RECIPIENT'S CATALOG NUMBER
4. TITLE (and Subtitle) A SIMPLE METHOD FOR PREDICTING MUZZLE BRAKE EFFECTIVENESS AND BAFFLE-SURFACE PRESSURE		5 TYPE OF REPORT & PERIOD COVERED Final
		6 PERFORMING ORG. REPORT NUMBER
7. AUTHOR(s) KEVIN S. FANSLER		8. CONTRACT OR GRANT NUMBER(s)
9. PERFORMING ORGANIZATION NAME AND ADDRESS U.S. Army Ballistic Research Laboratory (ATTN: DRDAR-BLL) Aberdeen Proving Ground, Maryland 21005		10 PROGRAM ELEMENT, PROJECT, TASK AREA & WORK UNIT NUMBERS RDT&E 1L161102AH43
11. CONTROLLING OFFICE NAME AND ADDRESS U.S. Army Armament Research & Development Command U.S. Army Ballistic Research Laboratory (ATTN: DRDAR-BL) Aberdeen Proving Ground, MD 21005		12. REPORT DATE JUNE 1981
		13 NUMBER OF PAGES 39
14. MONITORING AGENCY NAME & ADDRESS(if different from Controlling Office)		15. SECURITY CLASS. (of this report) Unclassified
		15a. DECLASSIFICATION/DOWNGRADING SCHEDULE

16. DISTRIBUTION STATEMENT (of this Report)

Approved for public release; distribution unlimited.

17. DISTRIBUTION STATEMENT (of the abstract entered in Block 20, if different from Report)

18. SUPPLEMENTARY NOTES

This report supersedes Interim Memorandum Report No. 696 dated December 1980.

19. KEY WORDS (Continue on reverse side if necessary and identify by block number)

Muzzle Brakes
Jet Flows
Brake Efficiency

20. ABSTRACT (Continue on reverse side if necessary and identify by block number) (ner)

The objective of this work is to produce a simple method for calculating load distributions on muzzle brake baffles during the firing process. With the load distribution known, the muzzle-brake effectiveness expression can be obtained and easily evaluated. The approach is to use a simple model for the muzzle-jet flow to predict the pressure on the baffle. The baffle is located in the supersonic jet core during much of the gun-exhaust cycle. This impinging flow onto the baffles is approximated by adopting a source flow model. Newtonian theory (Continued)

DD FORM 1473 1 JAN 73 EDITION OF 1 NOV 65 IS OBSOLETE

UNCLASSIFIED

SECURITY CLASSIFICATION OF THIS PAGE (When Data Entered)

UNCLASSIFIED

SECURITY CLASSIFICATION OF THIS PAGE(When Data Entered)

20. ABSTRACT (Continued):

is used to predict the resulting pressures on the baffles. The theoretical results compare well with previous published experimental results. With this model, brake-effectiveness variation with parameter changes can be simply obtained for most gun systems.

UNCLASSIFIED

SECURITY CLASSIFICATION OF THIS PAGE(When Data Entered)

TABLE OF CONTENTS

LIST OF ILLUSTRATIONS

PRECEDING PAGE BLANK-NOT FILMED

I. INTRODUCTION

A muzzle brake, Figure 1, is used to reduce the recoil of the gun thus allowing a lighter gun carriage. The impinging gun-exhaust plume exerts counterforces on the baffle surfaces thus reducing the recoil impulse. The cowls attach the baffles to the gun but may also affect the momentum imparted to the muzzle brake. The objective of this work is to calculate the muzzle-brake momentum index by a simple method. The momentum index value is a measure of the counter impulse given the brake compared to the gas ejection impulse and thus is a measure of the brake efficiency or effectiveness.

This work stems from the muzzle-brake investigations of Oswatitsch[1,2] and Smith[3,4]. Oswatitsch shows that the exhaust flow impinging upon a baffle may be approximated by a quasi-steady jet. Smith[3,4] also makes this assumption. Schmidt and Shear[5] have confirmed this hypothesis by utilizing optical techniques. Figure 2 displays the structure of the flow from the muzzle. Immediately after the projectile leaves the muzzle, the gases are freed to expand. The free-air blast forms and travels rapidly with the contact surface and Mach disc following. In the supersonic core, the gases expand from the high pressures at the muzzle to very low pressures near the barrel shock. Even through the Mach disc or blast front is moving, the region in the supersonic core approximates the flow in a steady jet with the same muzzle-exit conditions. With the baffle placed one to a few calibers away from the

---

1. *K. Oswatitsch, "Intermediate Ballistics," DVL R 358, Deutschen Versuchsanstalt für Luft-und Raumfahrt, Aachen, Germany, June 1964, (UNCLASSIFIED). AD 473 249.*

2. *K. Oswatitsch, "Flow Research to Improve the Efficiency of Muzzle Brakes, Part I-III," in Muzzle Brakes, Volume II: Theory, E. Hammer (ed.), Franklin Institute, Philadelphia, PA, 1949.*

3. *F. Smith, "Model Experiments on Muzzle Brakes," RARDE R 2/66, Royal Armament Research and Development Establishment, Fort Halstead, U.K., 1966. (UNCLASSIFIED). AD 487 121.*

4. *F. Smith, "Model Experiments on Muzzle Brakes, Part III: Measurement of Pressure Distribution," RARDE R 3/68, Royal Armament Research and Development Establishment, Fort Halstead, U.K., 1968. (UNCLASSIFIED). AD 845 519.*

5. *E. M. Schmidt and D. D. Shear, "Optical Measurement of Muzzle Blast," AIAA J., Vol. 13, No. 8, August 1975, pp. 1086-1091.*

muzzle, the baffle would be in the supersonic core for most of the gun exhaust phase. Thus, the core flow impinging upon the baffles primarily determines the momentum index.

In the present work, we first apply a simple theory for predicting pressures on the baffles given the impinging flow. With Schmidt, et al[6], and Smith[3,4], we utilize Newtonian theory. Next, we construct a simple model for the flow in the muzzle-jet plume assuming a supersonic source flow. With these assumptions, we then vary the source location so that the theoretical overpressure curve can be fitted to the experimental data of Schmidt, et al[6]. With the optimum source location established, the expression for the pressure can be integrated and a simple closed-form expression for the momentum-index of the brake is obtained.

The resulting model is applicable to most gun systems although the present study does not take into account how the efficiency varies with the amount of enclosure associated with the cowls. However, Smith's[3,4] experiments show the momentum-index changes little for small amounts of enclosure. Figure 3 shows that when δ, the angle that the disc is inclined from the radial plane, is equal to zero, (flat discs), the momentum index increases monotonically and almost linearly as the enclosure value for the cowls is increased. When the cowls enclose one-half of the surrounding space, the momentum-index increase is about 10%. When the angle δ is greater than 20°, the momentum index values go both below and above the value for the fully open brake. This maximum excursion when surrounding space is less than half closed by cowls is a little more than 5%.

II. MODEL FOR THE PRESSURE AND IMPINGING FLOW ONTO THE BAFFLE

The pressure on the baffle surface is calculated by Newtonian flow theory. Consider that the flow is incident on the baffle surface at the angle θ and with the local fluid velocity V. As fluid strikes the surface, the perpendicular component of momentum is dissipated but the velocity component tangent to the surface is unchanged. The resulting overpressure equation can be shown to be

$$p_s - p = \rho V^2 \sin^2\theta \qquad (1)$$

---

6. *E. M. Schmidt, E. J. Gion, and K. S. Fansler, "Measurement of Muzzle Blast and Its Impingement Upon Surfaces," AIAA 12th Fluid and Plasma Dynamics Conference, Williamsburg, VA, July 1979, AIAA Paper 79 - 1550.*

Here p_s is the pressure on the baffle and p is the local value of the pressure in the flow field. Schmidt, et al[6], applied this theory for gun-exhaust flow impinging upon a disc-baffle and obtained good agreement with experiment. They approximated the supersonic-core flow onto the baffle as a steady-jet method-of-characteristics calculation[7]. Smith[3] considers "that the flow which would normally pass through the disc is simply removed from the flow picture with a corresponding removal of its thrust component." This view, for a straight disc, is equivalent to the application of Newton's flow theory. Nevertheless, for conical baffles ($\delta > 0$), the two resulting expressions are somewhat different.

As discussed earlier, the flow onto the brake can be approximated as a steady supersonic jet-core flow with muzzle-exit conditions for the time of interest. Figure 4 shows a steady supersonic core flow generated by a method-of-characteristics calculation[7]. The lines going away from the muzzle are streamlines. The other set of lines are isoproperty lines along which the pressure, temperature and Mach number are constant. A feature of this flow structure permits a simplifying approximation. A short distance downstream of the muzzle, the streamlines tend to straighten out although still possessing some small curvature. Such a flow is reminiscent of the simpler supersonic source flow,which would have straight streamlines emanating from the center with the isoproperty lines represented by concentric circles. The source flow is defined if the position of the origin and the gasdynamic properties at a given radius are known.

Using Newtonian flow theory and the source flow approximation, we can derive a simple expression for the pressure on the surface of a baffle. We can start by restating that the flow field of a source flow can be determined if we know the position of the source point and the gasdynamic properties at a given radius. We will use the centerline properties to find the flow characteristics elsewhere in the field. We use a method of characteristics (MOC) scheme to generate the Mach number distribution along the boreline once and for all. This distribution approximates sufficiently well the distributions for a wide range of muzzle-exit conditions of interest. Figure 5 shows the Mach number distribution and other centerline properties for the jet core. Here the subscripts j and c denote the muzzle exit conditions and the local boreline conditions respectively. The symbols M and γ denote the Mach number and the specific heat ratio respectively.

---

7. *A. R. Vick, E. H. Andrews, J. S. Pennard, and C. B. Craidon, "Comparison of Experimental Free-Jet Boundaries with Theoretical Results Obtained with the Method of Characteristics," NASA Technical Note D-2327, June 1964 (NTIS N64-23032).*

The distance along the centerline is expressed in calibers. In fact, the distances in this paper will always be expressed in calibers. With the Mach number distribution and the muzzle exit conditions known, we can calculate the gasdynamic properties at any selected point on the centerline.

We then wish to know the local gasdynamic quantities, such as pressure, velocity, etc., located on a baffle surface. We first construct two spherical surfaces with the assumed source point as their centers. One surface intersects the impingement point and the other surface intersects the projection of the baffle's surface upon the boreline. The control surface is defined by the intersection of these surfaces with a differential cone having its vertex at the source point and its axis intersecting the impingement point. The local gasdynamic quantities at the surface intersecting the impingement point can be found by the momentum theorem since the local gasdynamic properties are known on the other spherical surface from an MOC calculation. Utilizing an approximation to the Newtonian pressure, Equation (1), an expression can then be obtained for the pressure on the baffle surface.

The foregoing brief description of the derivation is now described in more detail. Figure 6 shows the upper cross-section of a baffle and the end of the gun barrel. The origin of the source flow is along the boreline at a certain distance from the muzzle as shown in Figure 6. The angle δ is the angle that the disc is inclined from the radial plane, ϕ is the angle between the boreline and the flow direction at the baffle surface and θ is the angle of incidence of the impinging flow. With the source flow assumption, the circle defined by r is a property contour. In order to find the pressure at the given impingement point, we can construct a control volume from a differential area at the impingement point to a differential surface at r as shown in Figure 7. This control volume then comprises part of a differential cone volume extending from the source point to the impingement point on the baffle. The following relation is obtained for the momentum flux tensor in a control volume with steady flow:

$$\int (p\, n_i + \rho V_i\, V_j\, n_j) dS = 0 \qquad (2)$$

Here, standard indicial notation is used for vectors, and n_i is the ith component of the unit vector normal to the surface.[1] For the component along the flow direction, Equation (2) would yield

$$(p_c + \rho_c V_c^2)\, dS_5 = (p + \rho V^2)\, dS_6 + p_m\, (dS_6 - dS_5) \qquad (3)$$

Here the subscript c denotes the flow conditions along the centerline at z_1, and p_m denotes some value of p between r and r_1. The last term on the RHS of Equation (3) results from performing the integration over

the sides of the control surface. Since dS is proportional to r^2 and by the law of sines, $r_1/\sin\alpha = r/\sin\theta$:

$$\frac{dS_5}{dS_6} = \frac{\sin^2\theta}{\sin^2\alpha}$$

Equation (3) becomes, using the above equation and neglecting the relatively small RHS second term:

$$p + \rho V^2 = (p_c + \rho_c V_c^2)\frac{\sin^2\theta}{\sin^2\alpha} \tag{4}$$

Now in the flow of interest, we could approximate Equation (1) by

$$p_s \doteq (p + \rho V^2)\sin^2\theta \tag{5}$$

For baffle distances greater than 1 caliber from the muzzle, the error in the approximation to Equation (1) is small for the baffle configurations of interest. Substituting Equation (4) into Equation (5), we obtain in terms of ϕ and δ,

$$p_s = (p_c + \rho_c V_c^2)\cos^4(\phi-\delta)/\cos^2\delta \tag{6}$$

To transform Equation (6) to an easily calculated form, divide through by p_∞. Multiplying and dividing through by p_j, we obtain

$$\frac{p_s}{p_\infty} = \frac{p_s}{p_j}\frac{p_j}{p_\infty} \tag{7}$$

The value of p_j/p_∞ is estimated by interior ballistic theory. In terms of the Mach number of the flow, Equation (6) becomes, using Equation (7) together with the ideal gas law and the isentropic relations:

$$\frac{p_s}{p_\infty} = \frac{p_j}{p_\infty}\left(1 + \frac{\gamma-1}{2}M_j^2\right)^{\frac{\gamma}{\gamma-1}} F\,\frac{\cos^4(\phi-\delta)}{\cos^2\delta} \tag{8}$$

where M_j is the jet-exit Mach number and

$$F \equiv \frac{1 + \gamma M_c^{\,2}}{\left(1 + \frac{\gamma-1}{2} M_c^{\,2}\right)^{\frac{\gamma}{\gamma-1}}} \qquad (9)$$

The value of F as a function of distance in calibers along the boreline is shown in Figure 8. These values of F were calculated with a method-of-characteristics numerical scheme. It is found that F has negligible dependence on expected values of the muzzle-exit conditions M_j, γ and p_j/p_∞ for baffle positions of interest. For this analysis, F will be assumed to be independent of these muzzle-exit conditions. The thickness of the line comprises the differences observed for $\gamma = 1.2$ and $\gamma = 1.3$. These values of γ should cover the expected range of γ for propellant gases. Thus F is applicable to almost all gun systems.

Utilizing Schmidt et al[6], experimental data, the source point position may be varied to obtain optimum agreement with Equation (8). The expression for r as a function of z is the following:

$$r = 0.101z^2 + 0.528z + 0.271 + R_1 \tan \delta \qquad (10)$$

Here, R_1 is the projectile hole diameter expressed in calibers. Figure 9a gives the overpressure distribution on a disc that is located 1 caliber from the muzzle. The experiment used a disc with pressure gages inserted at half-caliber intervals along the radius of the disc. Comparisons between the experiment and the curve fit show good agreement. Figure 9b shows the comparison at 1.5 calibers. Figure 9c gives the comparison for the baffle positioned at 4 calibers. Here the agreement is not as good. It is impossible to move the source to a position to give a better fit. The calculated pressures are lower at the smaller radii, which agrees with the observations of Schmidt et al[6].

Although the model has been applied to a 20mm gun, the universality of the plume-flow characteristics permits the application of Equation (8) to most weapons. The model would appear to be less applicable as one encounters higher jet-exit Mach numbers. From the Mach contour lines and streamlines generated by the MOC calculations, the flow patterns indicate that the equivalent source would need to be moved farther from the muzzle as the jet-exit Mach number increased. Compared to the sonic jet, this would lower the pressures and also increase the fall-off rate of the pressures with increasing radius.

III. DEVELOPMENT OF MUZZLE-BRAKE MOMENTUM-INDEX EXPRESSION

As discussed in the Appendix, we have chosen the momentum index to be

$$\eta = \frac{I-I'}{G} \tag{11}$$

Here I is the recoil impulse of the gun-barrel with a bare muzzle, I' is the recoil impulse of the gun-barrel with the muzzle brake and G is the impulse given the bare-muzzle gun by the propellant gases. The gas impulse is essentially the time integral of the momentum flux passing the muzzle face of the gun. During the major portion of the gun-emptying phase, the ratio of the numerator to the denominator is approximately a constant, as shown in Appendix A. Thus, Equation (11) is well approximated by replacement of the time integrals by their corresponding integrands,

$$\eta = \frac{\int (p_s - p_\infty)\ n_z dS}{(p_j + \rho_j V_j^2) A_j} \tag{12}$$

Here dS is a differential surface on the muzzle brake and n_z is the z component of the unit vector normal to the surface. The denominator of Equation (12) is the thrust, T, generated by the propellant gas on the weapon and the numerator is simply $T-T'$ where T' is the thrust of the propellant gases with the muzzle brake in place. Equation (12) is then

$$\eta = 1 - \frac{T'}{T} \ .$$

If $T' = 0$, then all the exhaust thrust is canceled and $\eta = 1$. The momentum index thus gives a measure of the effectiveness or efficiency of the brake. Larger values of η indicate a more effective brake.

From Figure 6, we can show that dS in terms of ϕ and r is

$$dS = (2\pi r^2 \cos^2\delta \sin\phi\ d\phi)/\cos^3(\phi-\delta) \tag{13}$$

Substituting Equations (8) and (13) into Equation (12) with the value of p_∞ assumed small, we obtain

$$\eta = 2H \cos\delta \int \sin\phi \cos(\phi-\delta) d\phi \tag{14}$$

where

$$H = \frac{4r^2 \left(1 + \frac{\gamma-1}{2} M_j^2\right)^{\frac{\gamma}{\gamma-1}} F}{1 + \gamma M_j^2} \tag{15}$$

Integration of Equation (14) yields the momentum index expression

$$\eta = H \cos\delta \left\{ \cos\delta \ (\sin^2\phi_m - \sin^2\phi_n) + \right.$$

$$\left. \sin\delta \ [(\phi_m - \cos\phi_m \sin\phi_m) - (\phi_n - \cos\phi_n \sin\phi_n)] \right\} \quad (16)$$

Here the subscript "m" refers to the maximum value of the angle and "n" refers to the minimum value of the angle subtended by the muzzle brake. Of course, the total force on the baffle can be obtained by multiplying η by $p_j \ (1 + \gamma M_j^2) A_j$.

In keeping with the spirit of the preceding approximations and in view of the accuracy expected from this approach, a sufficiently good approximation to the calculated H is achieved using the following equation

$$H = 0.22 \ (z + R_1 \ \tan\delta) + 1.07 \quad (17)$$

The value of H is quite sensitive to the prescription for the source point placement. If the source point is moved toward the fixed baffle, the value of H is decreased. Nevertheless, the multiplicand of H in Equation (16) would be increased,thus partly offsetting a possible error made in source placement.

To illustrate how to use Equation (16) to calculate the momentum index, a program in BASIC is presented in Appendix B.

It should be noted that F can now be expressed in terms of Z, δ and the muzzle exit conditions. From Equation (15), we have

$$F = \frac{(1 + \gamma M_j^2) \qquad H}{4r^2 \ \left(1 + \frac{\gamma-1}{2} M_j^2\right)^{\frac{\gamma}{\gamma-1}}} \quad (18)$$

The value r is expressed in terms of z and δ according to Equation (10) and H is found from Equation (17). Thus the expression for the pressure, Equation (8), can now be found without resorting to the use of graphs or extensive calculations.

IV. DISCUSSION

It is of interest to see how far this analysis may be extended. For a variation of γ from 1.2 to 1.3, the value of H varies 1% for sonic jet-exit gas velocities. This result is obtained using a method-of-characteristics calculation with Equation (15). Furthermore, the Mach contours and lines of flow inclination vary little in this range of γ. Thus, we should be able to use Equation (16) for $1.2 < \gamma < 1.3$. The value of H varies more with the parameter M_j. The value of H increases by a factor of 1.35 from $M_j = 1$ to $M_j = 1.8$ and the optimum source-point location for agreement with experiment probably also changes. To see how the momentum index varies with M_j, we can utilize the approach of Schmidt[6] which describes the flow by MOC calculations. Figure 10 shows a comparison of η for different values of M_j at $z = 1.5$. The efficiency is found to vary little for the two values of M_j for discs of different radii. Thus, the model can at least be extended to the M_j range 1 to 1.8 for baffles in the vicinity of $z = 1.5$. Although the insensitivity of H to M_j undoubtedly occurs at other values of z, there may be less agreement than was displayed in Figure 10. For most cases, the value of M_j probably declines to near 1 early in the exhaust phase, so that the properly weighted value for M_j in Equation (12) would be close to 1. Taking into account this canceling behavior and the weighted value for M_j, the error should be small in assuming a sonic jet for most cases.

The model can also be compared to experiment for varying baffle angles. Figure 11 is a comparison between Smith's[3] experiments and the theory for baffles placed at $z = 1.5$. The efficiency increases with the baffle angle partly for the reason that the baffle is intercepting more of the flow. Smith's experiment was run for $\gamma = 1.67$ but Smith indicates that the results should be near the propellant-gas results where $\gamma = 1.25$.

It appears that the source-flow model can give approximate predictions of the momentum index for different design parameters of interest. Figure 12 explores the influence of the baffle angle, δ, on the momentum index for different values of baffle position. The outer and inner baffle radii are held constant. The momentum index increases little for larger values of δ at $z = 4$. In fact, the momentum index decreases slightly from $\delta = 30^{\circ}$ to $\delta = 40^{\circ}$.

It is of interest to find the distance for a certain diameter disc that would produce the highest momentum index. This might not be the best distance for placement since the brake mass and strength also have to be taken into consideration. Figure 13 shows how η varies with z for different radii of discs using the present model.

The model results are compared with the experimental results of Smith. For the limited amount of data available, the agreement between experiment and theory is good. Both the model and experiment show that η decreases as z decreases for small values of z. This occurs because an increasing amount of the flow is going through the projectile hole. At large values of z, less of the flow intercepts the brake baffle as z increases. The maximum value of η occurs at larger values of z as the disc radius increases. The effect of the projectile hole loss becomes apparent at larger values of z as the radius of the disc is increased. The maximum values for the experimental curves occur at slightly larger values of z than the model predicts.

V. SUMMARY AND CONCLUSIONS

A simple method for calculating the pressures on the baffle and the impulse given the muzzle brake during firing has been developed. The method utilizes Newtonain flow theory and a source flow whose origin is moved with baffle distance to provide optimum agreement with experimental results. Although the method was developed using one weapons system, the model can be applied to most gun systems. Application of the method requires knowledge of the size of the disc and projectile hole, distance of the projectile hole from the muzzle and the angle δ. Additionally, to obtain baffle pressures, knowledge of the muzzle-exit conditions is required. The momentum index is calculated using a simple formula. The results agree well with an independent experiment[3,4].

Although the method was developed specifically for disc baffles and sonic muzzle jets, the method can be extended to more complex muzzle-brake shapes and often to muzzle flow with initial supersonic exit conditions. Some baffle shapes could be approximated by a collection of discs and sections of discs. For disc baffles, Smith[3] indicates cowling enclosing the surrounding space by less than one-half seems to change the momentum index by only a small amount. Nevertheless, comparing the present method's calculations with results[8] for rectangular baffle plates using top and bottom plates, we find that the present method's momentum index values are lower. The average values obtained by the present method need to be multiplied by 1.3 to agree with the average experimental values. It is assumed that this discrepancy is caused by the effect of the top and bottom plates.

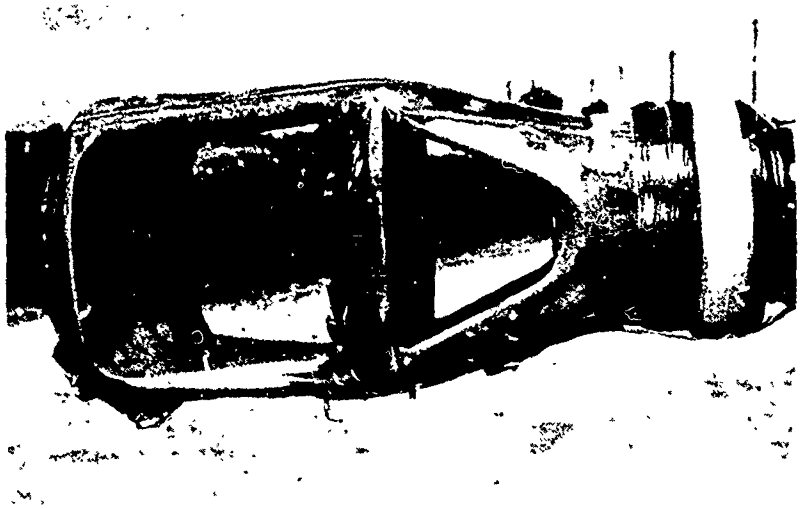

Figure 1. Double-Baffle Muzzle Brake with Instrumentation

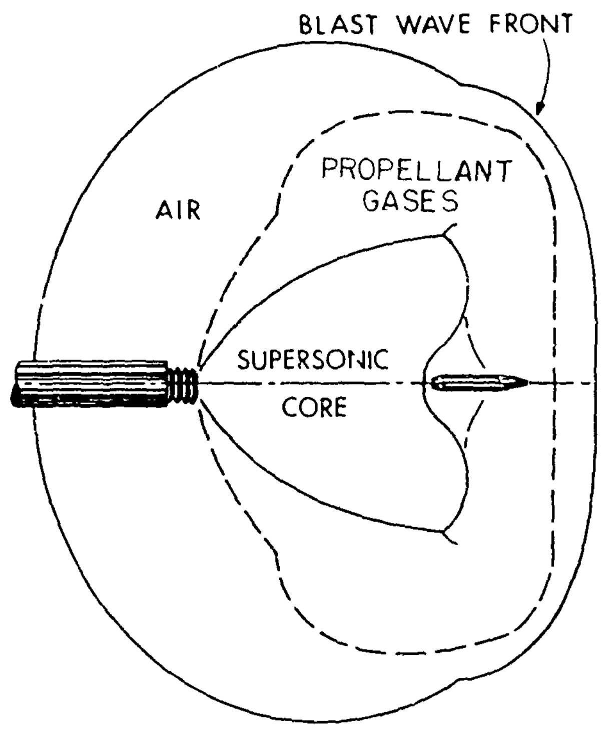

Figure 2. Flow Structure of the Gun Blast

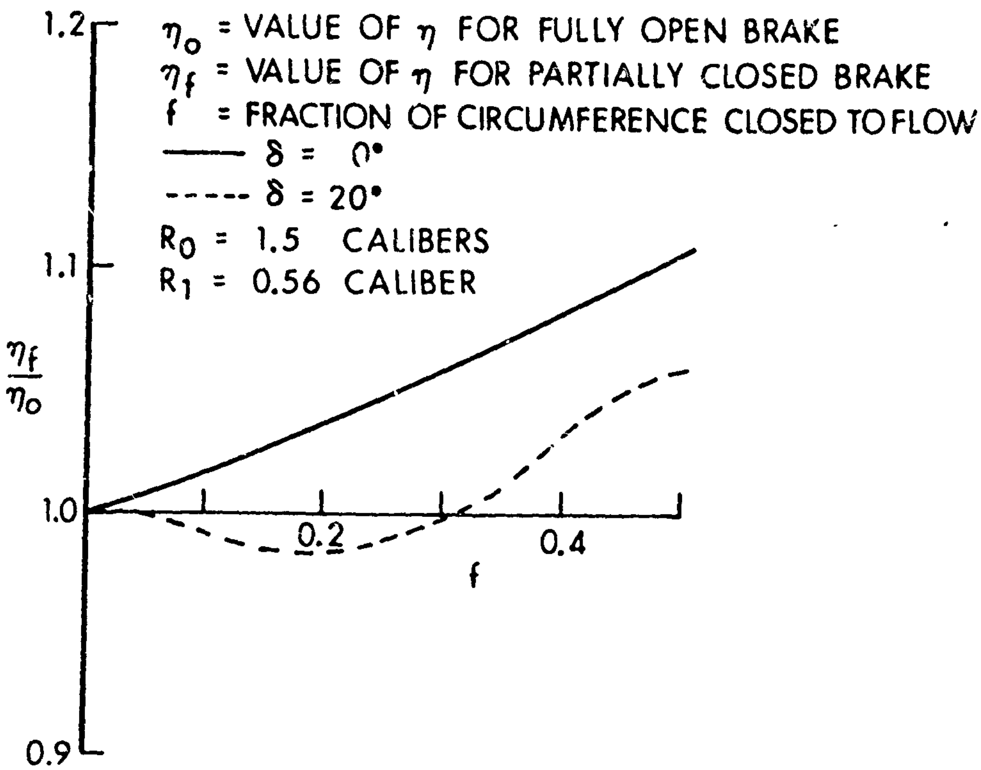

Figure 3. Effect of Partially Closing a Brake

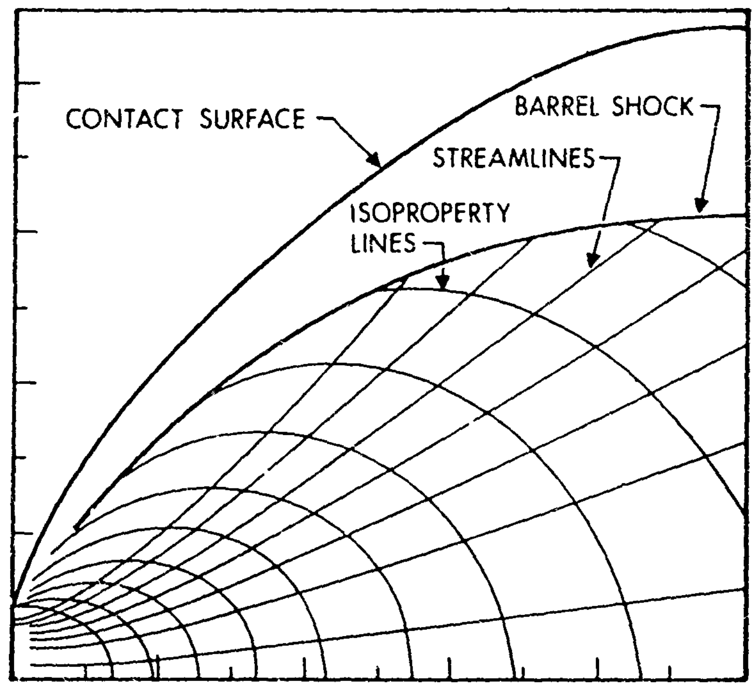

Figure 4. Streamlines and Isoproperty Lines for Steady Jet

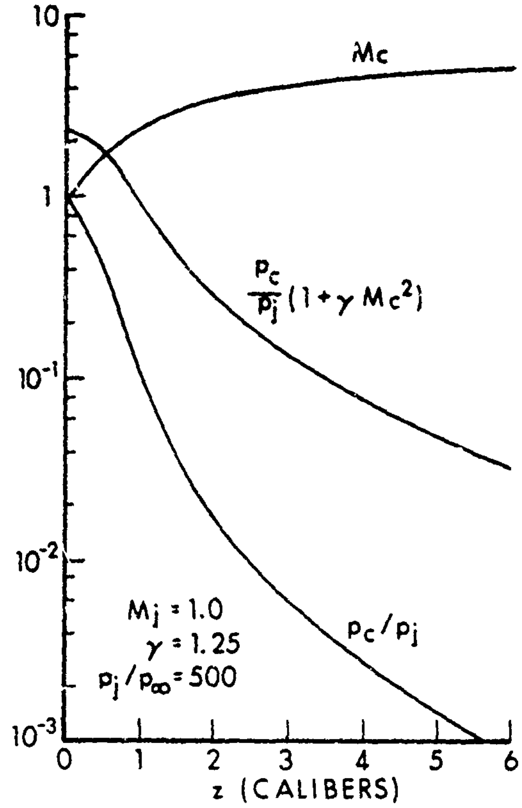

Figure 5. Some Centerline Property Distributions for the Jet Core

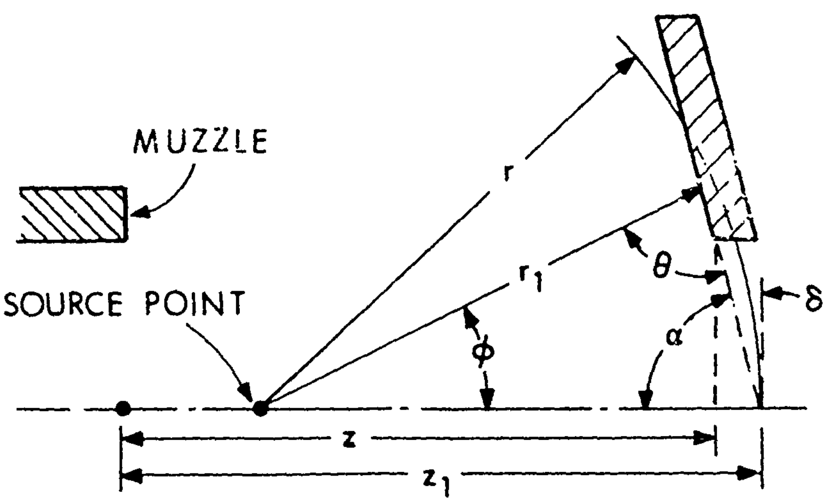

Figure 6. Illustrating Source Flow Impingement onto Baffle

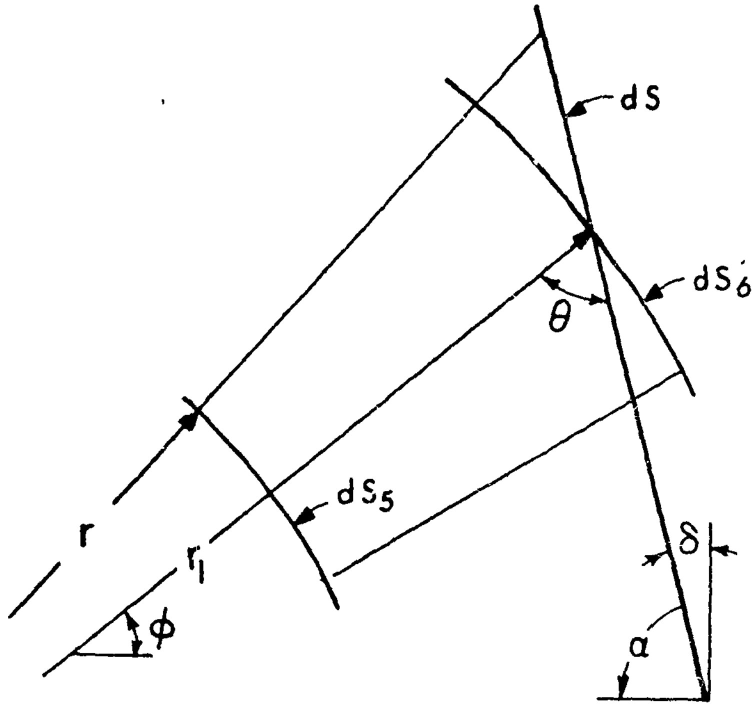

Figure 7. Illustrating Cone-Section Control Volume Located next to the Baffle Surface

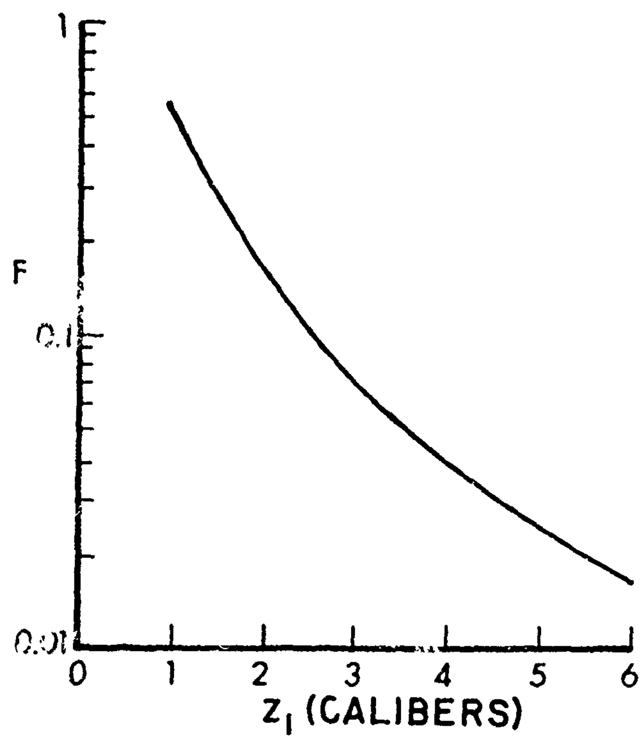

Figure 8. Jet Property Function on Boreline

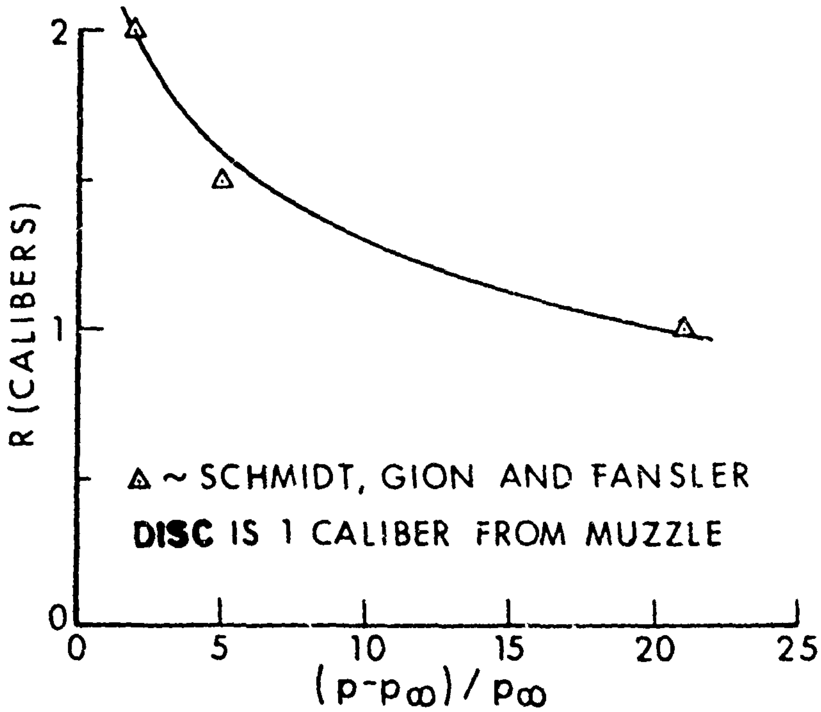

Figure 9a. Comparison of Optimized Model with Experiment (z = 1 caliber)

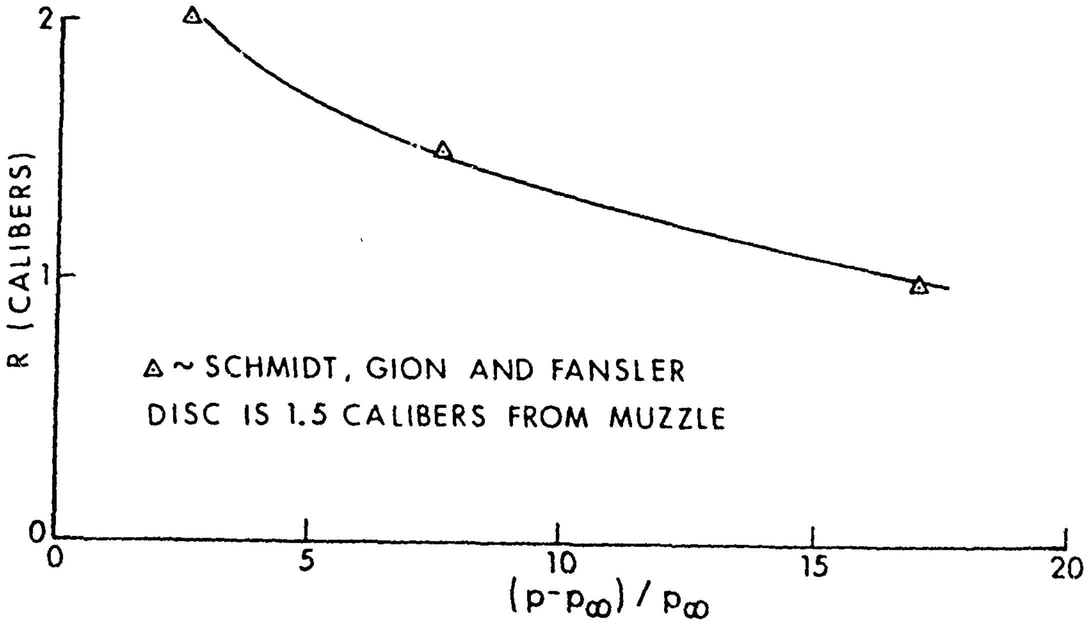

Figure 9b. Comparison of Optimized Model with Experiment (z = 1.5 calibers)

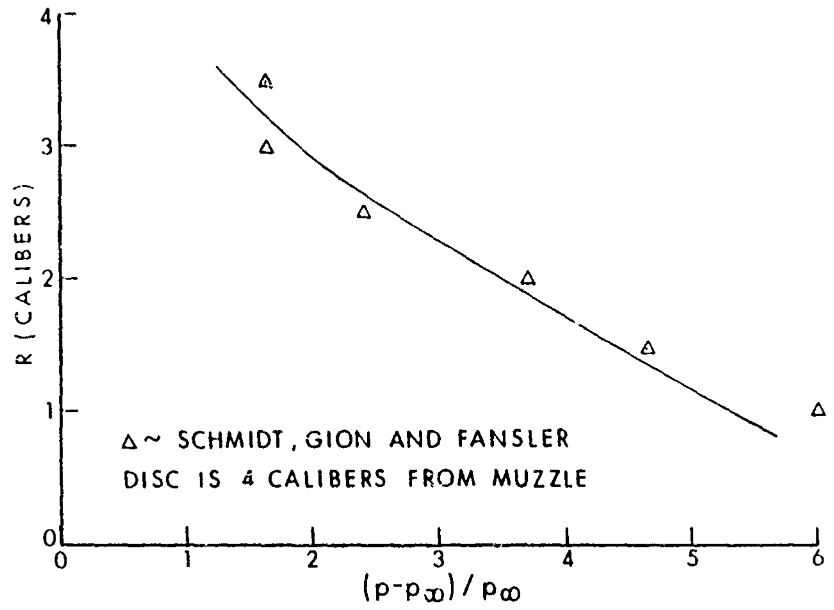

Figure 9c. Comparison of Optimized Model with Experiment (z = 4 calibers)

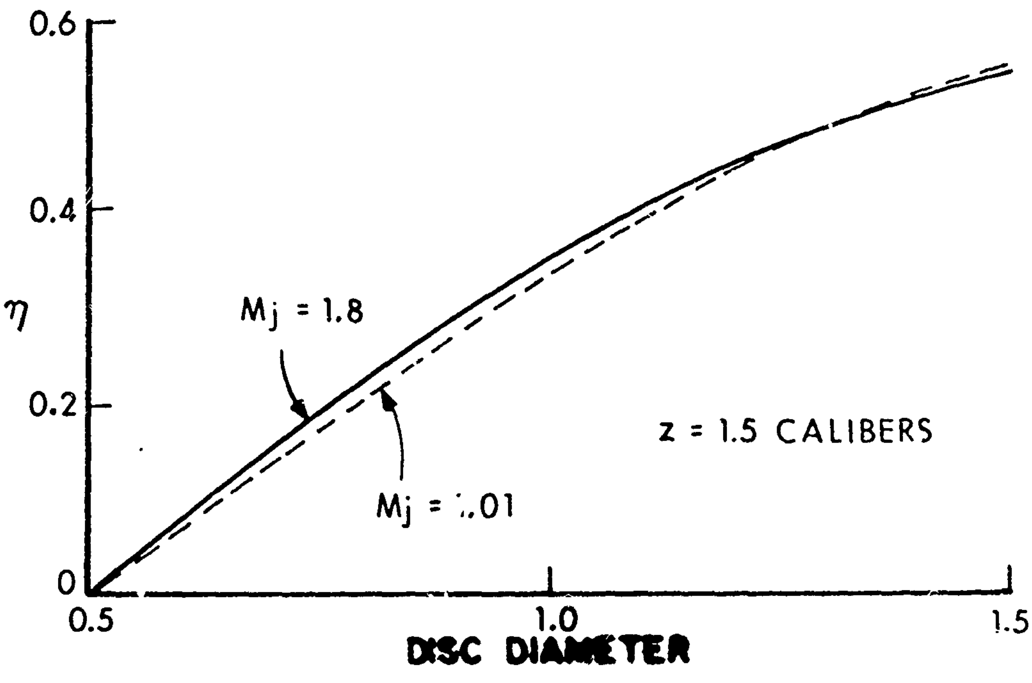

Figure 10. Momentum Index Comparison for Different Muzzle-Exit Mach Numbers

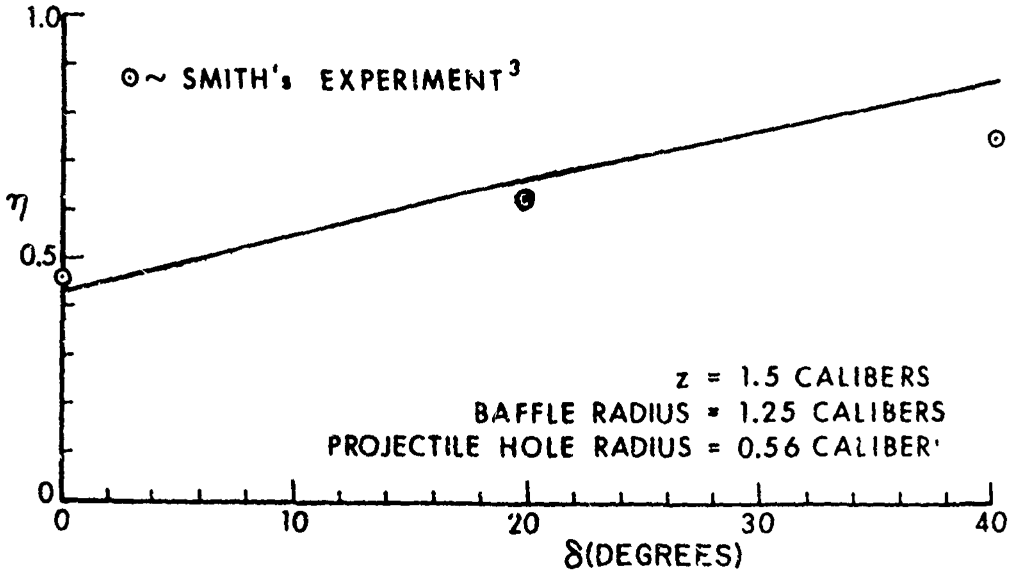

Figure 11. Momentum Index versus Baffle Angle; Comparison Between Theory and Experiment

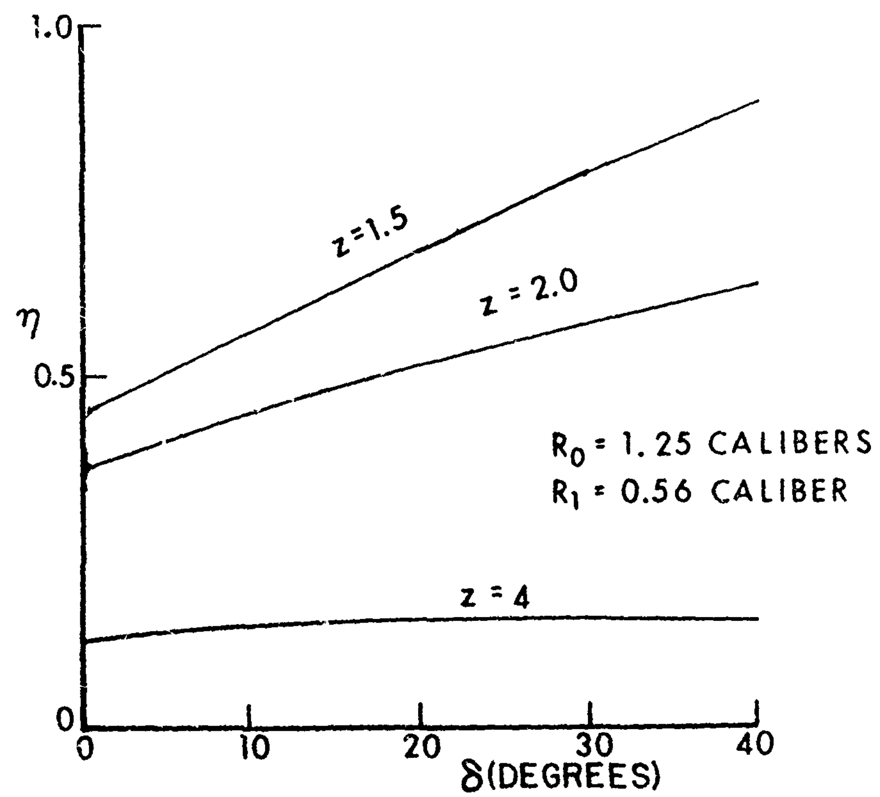

Figure 12. Momentum Index versus Baffle Angle for Different Baffle Distances

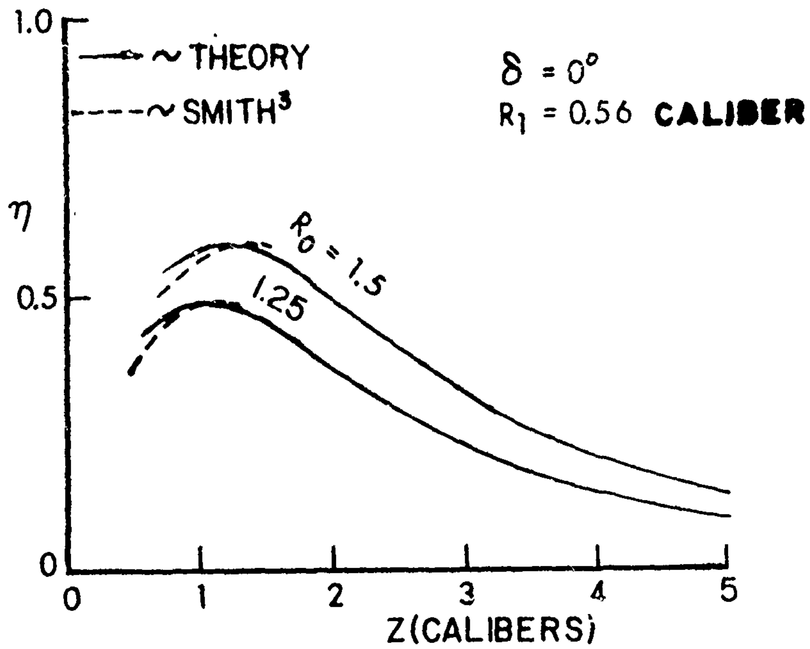

Figure 13. Momentum Index versus Baffle Position; Comparison Between Theory and Experiment

REFERENCES

1. K. Oswatitsch, "Intermediate Ballistics," DVL R 358, Deutschen Versuchsanstalt für Luft-und Raumfahrt, Aachen, Germany, June 1964, (UNCLASSIFIED). AD 473 249.

2. K. Oswatitsch, "Flow Research to Improve the Efficiency of Muzzle Brakes, Parts I-III," in Muzzle Brakes, Volume II: Theory, E. Hammer (ed.), Franklin Institute, Philadelphia, PA, 1949.

3. F. Smith, "Model Experiments on Muzzle Brakes," RARDE R 2/66, Royal Armament Research and Development Establishment, Fort Halstead, U.K., 1966. (UNCLASSIFIED). AD 487 121.

4. F. Smith, "Model Experiments on Muzzle Brakes, Part III: Measurement of Pressure Distribution," RARDE R 3/68, Royal Armament Research and Development Establishment, Fort Halstead, U.K., 1968. (UNCLASSIFIED). AD 845 519.

5. E. M. Schmidt and D. D. Shear, "Optical Measurement of Muzzle Blast," AIAA J., Vol. 13, No. 8, August 1975, pp. 1086-1091.

6. E. M. Schmidt, E. J. Gion, and K. S. Fansler, "Measurement of Muzzle Blast and Its Impingement Upon Surfaces," AIAA 12th Fluid and Plasma Dynamics Conference, Williamsburg, VA, July 1979, AIAA Paper 79 - 1550.

7. A. R. Vick, E. H. Andrews, J. S. Pennard, and C. B. Craidon, "Comparison of Experimental Free-Jet Boundaries with Theoretical Results Obtained with the Method of Characteristics," NASA Technical Note D-2327, June 1964 (NTIS N64-23032).

8. L. L. Pater, "Muzzle Brake Parameter Study," NSWC/DL TR-3531, U. S. Naval Surface Weapons Center, Dahlgren Laboratory, Dahlgren, VA 22448, October 1976, (UNCLASSIFIED).

APPENDIX A. MUZZLE BRAKE EFFECTIVENESS DEFINITIONS

The muzzle-brake effectiveness parameter gives a measure of the recoil reduction of the muzzle brake. There are various definitions for muzzle brake effectiveness. Arguments have been made concerning the best definition to use. In this Appendix we attempt to show the advantages of our definition.

We start by considering the momentum given the gun during the firing process. We neglect friction processes, and write Newton's Second Law as

$$\frac{d}{dt}\int \rho V_i \, d\tau = -\int p n_i \, dS \qquad \text{(A-1)}$$

This equation is in indicial notation. Here $d\tau$ is a volume element, dS is an element of the surface chosen and n_i is a component of the unit vector normal to and pointing out from the control surface. This expression can be manipulated to

$$M_p \frac{d}{dt} V_p + \frac{\partial}{\partial t}\int \rho V_i \, d\tau = -\int (p n_i + \rho V_i V_k n_k) \, dS \qquad \text{(A-2)}$$

Here M_p and V_p are the mass and velocity of the projectile respectively. Placing the control surface along the interior surface of the gun and across the surface of a bare muzzle gun, we obtain for times before shot ejection

$$\int p_b dS_b - \int p dS_S n_z = \int (p_j + \rho_j V_j^2) \, dA_j + \frac{\partial}{\partial t}\int \rho V_z \, d\tau + M_p \frac{d}{dt} V_p \qquad \text{(A-3)}$$

Here the subscript j denotes exit conditions, V_z is the z-component of the velocity, the subscript b refers to the interior base of the gun barrel, the subscript S refers to the sides of the tube and dA_j refers to the element of surface at the gun muzzle. The propellant gas and the precursor gas are included in the element $d\tau$ in the second term on the RHS of Equation (A-3). Now assume that the gas dynamic conditions do not vary radially. The total recoil impulse can be obtained by subtracting p_∞ from both sides of Equation (A-3) and integrating with respect to time:

$$I = A_j \int_{-\infty}^{+\infty} (p_j - p_\infty + \rho_j V_j^2) \, dt + m_p V_p + \iint_{-\infty}^{+\infty} \frac{\partial}{\partial t} (\rho V d\tau) dt \qquad \text{(A-4)}$$

Here, $t = 0$ corresponds to the time at shot ejection. The last term,

PRECEDING PAGE BLANK-NOT FILMED

when evaluated at $t = \pm \infty$, drops out. The impulse for the gun with the muzzle brake is

$$I' = I - \int_{-\infty}^{+\infty} [\int (p_s - p_\infty)\, n_z \, dS]\, dt \qquad \text{(A-5)}$$

where the integrand is integrated over the brake surface, S, and p_s is the pressure on the brake surface.

The momentum index can be defined as

$$\eta \equiv \frac{I - I'}{G} \qquad \text{(A-6)}$$

where G is the impulse given the gun by the propellant gases

$$G \equiv I - m_p V_p \qquad \text{(A-7)}$$

Thus, the momentum index becomes

$$\eta = \frac{\int [\int (p_s - p_\infty)\, n_z \, dS]\, dt}{G} \qquad \text{(A-8)}$$

The flow pattern in the jet varies little with the jet-exit pressures of interest. Over the range of jet-exit pressures of interest, the integrand part of the numerator should be proportional to the muzzle-exit pressure and the integrand in the denominator is also proportional to the jet-exit pressure. Furthermore, results obtained by MOC calculations and application of Newtonian theory show that the ratio of the integrands in Equation (A-8) is only weakly dependent upon the initial jet-exit Mach number. The momentum index can then be approximated by

$$\eta \doteq \frac{\int (p_s - p_\infty)\, n_z \, dS}{(p_j + \rho_j V_j^{\,2})\, A_j} \qquad \text{(A-9)}$$

The exit properties would be weighted so that they represent times shortly after shot ejection when muzzle pressures were comparable to the peak muzzle pressure. The flow pattern should be only very weakly dependent on charge and projectile masses. The value of η should also be very weakly dependent on the initial muzzle exit conditions. Hence, η should depend primarily on the muzzle-brake configuration.

The experimental determination of η is rather straightforward. One simply determines I and I' with an impulse measuring machine. The projectile mass and velocity of the projectile can also be measured with some accuracy. The value of G is easily determined by Equation (A-7). The value of the momentum index is then determined by substituting experimental values into Equation (A-6). The expression for η, Equation (A-9), also lends itself well to theoretical analysis.

L. L. Pater[8] has defined a similar momentum index except that G is replaced by I_a, "defined as that portion of the total recoil impulse which occurs after projectile ejection." This value of the impulse would be, using Equation (A-4) and (A-7) but evaluating at t = 0 instead of at t = +∞,

$$I_a = G - A_j \int_{-L}^{o} \rho V dz - A_j \int_{-\infty}^{o} (p_j - p_\infty + \rho_j V_j^2)\, dt.$$

Here L is the length of the barrel in calibers. The third term involves the flow of precursor gases out of the barrel and, in most cases, would be small compared to the other terms. There are two difficulties with using I_a. First, one must make an assumption about the distributions of ρ and V inside the barrel at the time of shot ejection since they are not known. This can lead to some experimental and theoretical uncertainties. Second, for this definition of momentum index to be invariant to charge weights, projectile weights and barrel length, the second and third terms must be directly proportional to the corresponding values for G. It is not at all obvious to the author that this would be the case although L. L. Pater noted that in his experiments, his momentum index for a given muzzle brake varied little with the different gun parameters he used.

There are other definitions for measures of muzzle brake effectiveness. L. L. Pater[8] discusses these in some detail in his report. He shows that they all seem to have some drawbacks that limit their usefulness.

---

8. *L. L. Pater, "Muzzle Brake Parameter Study," NSWC/DL TR-3531, U.S. Naval Surface Weapons Center, Dahlgren Laboratory, Dahlgren, VA 22448, October 1976, (UNCLASSIFIED).*

APPENDIX B. PROGRAM FOR CALCULATING THE PRESSURE AND THE MOMENTUM INDEX

Below is a computer program coded in BASIC that, given the projectile hole radius and outer baffle radius, can calculate the momentum index either as a function of baffle distance from muzzle or the baffle angle, δ. It can also calculate the pressure field on a baffle.

```
100 REM PROGRAM TO FIND MOMENTUM INDEX OR PRESSURE ON BAFFLE
110 PRINT "DO YOU WANT TO CALCULATE THE PRESSURE?"
120 INPUT B$
130 IF B$="Y" THEN 660
140 PRINT "INPUT THE PROJECTILE HOLE RADIUS IN CALIBERS"
150 REM R1 IS SMALLEST RADIUS
160 INPUT R1
170 REM R0 IS THE MAXIMUM RADIUS OF THE BAFFLE
180 PRINT "INPUT THE BAFFLE RADIUS IN CALIBERS"
190 INPUT R0
200 PRINT "DO YOU WANT TO CALCULATE MOMENTUM INDEX IN TERMS OF Z"
210 PRINT "ANSWER BY PRESSING EITHER Y OR N"
220 INPUT A$
230 IF A$="Y" THEN 330
240 PRINT "INPUT THE DISTANCE,Z, TO BAFFLE IN CALIBERS"
250 INPUT Z
260 PRINT "TO START OVER, INPUT THE VALUE 100"
270 PRINT "INPUT THE ANGLE IN DEGREES"
280 INPUT D
290 IF D=>100 THEN 140
300 I=1
310 GO TO 420
320 REM D IS THE BAFFLE DISH ANGLE(DEGREES)
330 PRINT "INPUT THE ANGLE DELTA IN DEGREES"
340 INPUT D
350 REM Z IS DISTANCE FROM MUZZLE TO RADIAL PROJECTION OF R1 ONTO AXIS
360 PRINT "TO START OVER, INPUT THE VALUE 100"
370 PRINT "INPUT THE DISTANCE,Z, TO BAFFLE IN CALIBERS"
380 INPUT Z
390 IF Z=>100 THEN 140
400 I=0
410 REM THE ANGLE "DELTA" IN TERMS OF RADIANS
420 D1=PI*D/180
430 REM Z6 IS A RESULT OF AN INTERMEDIATE CALCULATION
```

```
440 Z6=0.271+0.528*Z+0.101*Z↑2
450 REM Z5 IS A DISTANCE GIVEN AS "r" IN REPORT
460 Z5=Z6+R1*TAN(D1)
470 REM ANGLE IN REPORT CORRESPONDING TO R1
480 F1=ATN(R1/(Z5-R1*TAN(D1)))
490 REM ANGLE IN REPORT CORRESPONDING TO R0
500 F0=ATN(R0/(Z5-R0*TAN(D1)))
510 C1=COS(F1)
520 S1=SIN(F1)
530 C0=COS(F0)
540 S0=SIN(F0)
550 C2=COS(D1)
560 S2=SIN(D1)
570 REM H AS DEFINED IN REPORT
580 H=1.07+0.22*(Z+R1*TAN(D1))
590 T1=F1-C1*S1
600 T0=F0-C0*S0
610 REM E IS THE MOMENTUM INDEX AS DEFINED IN REPORT
620 E=H*C2*(C2*(S0↑2-S1↑2)+S2*(T0-T1))
630 PRINT D,Z,E
640 IF I=1 THEN 280
650 GO TO 380
660 PRINT "INPUT THE MUZZLE EXIT PRESSURE IN ATMOSPHERES"
670 INPUT P1
680 PRINT "INPUT THE JET EXIT MACH NUMBER"
690 INPUT M1
700 PRINT "INPUT DISTANCE FROM MUZZLE TO BAFFLE"
710 INPUT Z
720 PRINT "INPUT THE BAFFLE ANGLE,DELTA, IN DEGREES"
730 INPUT D
740 PRINT "INPUT THE PROJECTILE HOLE RADIUS IN CALIBERS"
750 INPUT R1
760 PPINT "TO START OVER, INPUT THE VALUE 100"
770 PRINT "INPUT THE RADIAL POSITION OF THE BAFFLE IMPINGEMENT POINT"
780 INPUT R
790 IF R=-100 THEN 100
800 REM THE ANGLE "DELTA" IN TERMS OF RADIANS
810 D1=PI*D/180
820 REM Z6 IS A RESULT OF AN INTERMEDIATE CALCULATION
830 Z6=0.271+0.528*Z+0.101*Z↑2
840 REM Z5 IS A DISTANCE GIVEN AS "r" IN REPORT
850 Z5=Z6+R1*TAN(D1)
860 REM ANGLE "PHE" IN REPORT CORRESPONDING TO R
870 P8=ATN(R/(Z5-R*TAN(D1)))
880 REM Z1 IS AS DEFINED IN REPORT
890 Z1=Z+R1*TAN(D1)
900 REM H IS AS DEFINED IN REPORT
910 H=0.22*Z1+1.07
920 REM F IS AS DEFINED IN REPORT
930 F=1.25*H/4/Z5/Z5
940 REM INTERMEDIATE CALCULATION
950 I1=(1+M1*M1/8)↑5
960 REM EXPRESSION FOR PRESSURE ON SURFACE OF BAFFLE
970 P=P1*I1*F*COS(P8-D1)↑4/COS(D1)↑2
980 REM
990 P2=P-1
1000 REM THE ANGLE "PHE" IN DEGREES
1010 P9=180*P8/PI
1020 REM
1030 REM
1040 PRINT R,P9,F,P2
1050 GO TO 780
1060 END
1070 REM
```

LIST OF SYMBOLS

A	Area of gun bore
f	fraction of cylindrical surface defined by R_o, the muzzle plane, and plane intersecting baffle outer radius that is closed by cowling
F	dimensionless factor in expression for baffle-pressure
G	propellant-gas impulse given gun without muzzle brake
H	dimensionless factor in momentum index expression that is dependent on baffle position
I	recoil impulse without baffle
I_a	propellant-gas impulse defined by Pater
I'	recoil impulse with baffle
m_p	mass of projectile
M	local Mach number in flow
M_c	centerline Mach number at z_1 (refer to Figure 6)
M_j	Mach number at jet exit
p_s	pressure on baffle surface
p_c	jet centerline static pressure at z_1
p_j	static pressure at jet exit
p	local pressure in jet
p_∞	ambient pressure
r	distance from source point to the intersection point of the baffle plane with the boreline expressed in calibers
r_1	distance from source point to a point on the baffle surface expressed in calibers
R	radial position on baffle surface
R_o	outer radius of baffle expressed in calibers

LIST OF SYMBOLS (Continued)

R_1	projectile hole radius expressed in calibers
S	surface to be integrated
t	time with respect to projectile uncorking
T	thrust given to gun by propellant gases
V	local fluid velocity
V_c	jet velocity along centerline at z_1
V_p	velocity of projectile
z	position of baffle with respect to muzzle expressed in calibers
z_1	distance from muzzle to the intersection point of baffle plane expressed in calibers
α	angle that the baffle surface makes with the boreline
γ	specific heat ratio
δ	angle that the disc is inclined from the radial plane
ρ	local fluid density in jet
ρ_c	local fluid density along centerline at z_1
θ	angle of incidence for gas flow onto plate
ϕ	angle between boreline direction and flow direction at the baffle surface
η	momentum index defined by Equation (11)

DISTRIBUTION LIST

No. of Copies	Organization
12	Commander Defense Technical Info Center ATTN: DDC-DDA Cameron Station Alexandria, VA 22314
1	Director Defense Nuclear Agency Washington, DC 20305
2	HQDA (DAMA-WSA, MAJ Csoka; DAMA-CSM, LTC Germann) Washington, DC 20310
1	Director US Army BMD Advanced Technology Center P. O. Box 1500, West Station Huntsville, AL 35807
1	Commander US Army Ballistic Missile Defense Systems Command Huntsville, AL 35804
1	ODCSI, USAREUR & 7A ATTN: AEAGB-PDN (S&E) APO, New York 09403
1	Commander US Army Materiel Development and Readiness Command ATTN: DRCDMD-ST 5001 Eisenhower Avenue Alexandria, VA 22333
1	Commander US Army Materiel Development and Readiness Command ATTN: DRCDL 5001 Eisenhower Avenue Alexandria, VA 22333
7	Commander US Army Armament Research and Development Command ATTN: DRDAR-TSS (2 cys) DRDAR-TDS, Mr. Lindner DRDAR-TDA, Mr. Blick DRDAR-LC-F, Mr. A. Loeb Mr. E. Friedman DRDAR-SEM W. Bielauskas Dover, NJ 07801
6	Commander US Army Armament Research and Development Command ATTN: DRDAR-LCV, Mr. Reisman DRDAR-SCN, Mr. Kahn DRDAR-LC, Dr. Frasier DRDAR-SCW, Mr. Townsend DRDAR-SG, Dr. T. Hung PM, XM788/789, LTC Delany Dover, NJ 07801
1	Commander US Army Armament Materiel Readiness Command ATTN: DRSAR-LEP-L, Tech Lib Rock Island, IL 61299
6	Director US Army ARRADCOM Benet Weapons Laboratory ATTN: DRDAR-LCB-TL Mr. W. Dock Dr. G. Carofano Mr. P. Alto DRDAR-LCB, Mr. T. Allen Mr. R. Billington Watervliet, NY 12189

DISTRIBUTION LIST

No. of Copies	Organization
3	Commander US Army Aviation Research and Development Command ATTN: DRSAV-E DRCPM-AAH Product Manager, AH-1 P. O. Box 209 St. Louis, MO 63166
1	Director US Army Air Mobility Research and Development Laboratory Ames Research Center Moffett Field, CA 94035
1	Commander US Army Communications Rsch and Development Command ATTN: DRDCO-PPA-SA Fort Monmouth, NJ 07703
1	Commander US Army Electronics Research and Development Command Technical Support Activity ATTN: DELSD-L Fort Monmouth, NJ 07703
6	Commander US Army Missile Command ATTN: DRSMI-R DRSMI-RBL DRSMI-RDK DRSMI-YDL (2 cys) Redstone Arsenal, AL 35809
1	Commander US Army Natick Research and Development Command ATTN: DRXRE, Dr. D. Sieling Natick, MA 01762
1	Commander US Army Tank Automotive Research & Development Cmd ATTN: DRDTA-UL Warren, MI 48090
1	Commander US Army Jefferson Proving Ground ATTN: STEJP-TD-D Madison, IN 47250
1	Commander US Army Materials and Mechanics Research Center ATTN: DRXMR-ATL Watertown, MA 02172
1	Commander US Army Research Office ATTN: CRD-AA-EH P. O. Box 12211 Research Triangle Park NC 27709
2	Director US Army TRADOC Systems Analysis Activity ATTN: ATAA-SL, Tech Lib ATAA-S White Sands Missile Range NM 88002
3	Commander Naval Air Systems Command ATTN: AIR-604 Washington, DC 20360
3	Commander Naval Ordnance Systems Command ATTN: ORD-9132 Washington, DC 20360

DISTRIBUTION LIST

No. of Copies	Organization
2	Commander and Director David W. Taylor Naval Ship Research & Development Cmd ATTN: Lib Div, Code 522 Aerodynamic Lab Bethesda, MD 20084
1	Commander Naval Surface Weapons Center ATTN: Code 730, Tech Lib Silver Spring, MD 20910
1	Commander Naval Weapons Center ATTN: Code 553, Tech Lib China Lake, CA 93555
1	Commander Naval Research Laboratory ATTN: Tech Info Div Washington, DC 20375
1	Commander Naval Ordnance Station ATTN: Code FS13A, P. Sewell Indian Head, MD 20640
1	AFRPL/LKCB, Dr. Horning Edwards AFB, CA 93523
2	AFATL (DLDL, D.C. Daniel; Tech Lib) Eglin AFB, FL 32542
3	Commander Naval Surface Weapons Center ATTN: Code 6X Mr. F. H. Maille Dr. J. Yagla Dr. G. Moore Dahlgren, VA 22448
1	AFWL/SUL Kirtland AFB, NM 87117
1	ASD/XRA (Stinfo) Wright-Patterson AFB, OH 45433
1	Director National Aeronautics and Space Administration George C. Marshall Space Flight Center ATTN: MS-I, Lib Huntsville, AL 38512
1	Director Jet Propulsion Laboratory ATTN: Tech Lib 2800 Oak Grove Drive Pasadena, CA 91103
1	Director National Aeronautics and Space Administration Langley Research Center ATTN: MS 185, Tech Lib Langley Station Hampton, VA 23365
1	Director NASA Scientific and Technical Information Facility ATTN: SAK/DL P. O. Box 8757 Baltimore/Washington International Airport, MD 21240
1	AAI Corporation ATTN: Dr. T. Stastny Cockeysville, MD 21030

DISTRIBUTION LIST

No. of Copies	Organization
1	Advanced Technology Labs ATTN: Mr. J. Ranlet Merrick & Steward Avenues Westbury, NY 11590
1	Aerospace Corporation ATTN: Dr. T. Taylor P. O. Box 92957 Los Angeles, CA 90009
1	ARO, Inc. ATTN: Tech Lib Arnold AFS, TN 37389
1	ARTEC Associates, Inc. ATTN: Dr. S. Gill 26046 Eden Landing Road Hayward, CA 94545
2	AVCO Systems Division ATTN: Dr. W. Reinecke Dr. D. Siegelman 201 Lowell Street Wilmington, MA 01887
1	Battelle Columbus Laboratories ATTN: J. E. Backofen, Jr. 505 King Avenue Columbus, OH 43201
1	Technical Director Colt Firearms Corporation 150 Huyshope Avenue Hartford, CT 14061
1	Flow Simulations Inc. ATTN: Dr. J. Steger 735 Alice Ave Mountain View, CA 94041
1	ARO, Inc. Von Karman Gasdynamics Facility ATTN: Dr. J. Adams Arnold AFS, TN 37389
2	General Electric Corporation Armaments Division ATTN: Mr. R. Whyte Mr. J. MacNeil Lakeside Avenue Burlington, VT 05401
1	Honeywell, Inc. ATTN: Mail Station MN 112190 (G. Stilley) 600 Second Street, North Hopkins, MN 55343
3	Hughes Helicopter Company Bldg. 2, MST22B ATTN: Mr. R. Forker Mr. T. Edwards Mr. R. Flood Centinella and Teel Streets Culver City, CA 90230
1	Martin Marietta Aerospace ATTN: Mr. A. J. Culotta P. O. Box 5387 Orlando, FL 32805
1	Winchester-Western Division Olin Corporation New Haven, CT 06504
1	Rockwell Int'l Science Center ATTN: Dr. Norman Malmuth P. O. Box 1085 1000 Oaks, CA 91360
1	Sandia Laboratories ATTN: Aerodynamics Dept Org 5620, R. Maydew Albuquerque, NM 87115
1	S&D Dynamics, Inc. ATTN: Dr. M. Soifer 755 New York Avenue Huntington, NY 11743

DISTRIBUTION LIST

No. of Copies	Organization
1	Guggenheim Aeronautical Lab California Institute of Tech ATTN: Tech Lib Pasadena, CA 91104
1	Franklin Institute ATTN: Tech Lib Race & 20th Streets Philadelphia, PA 19103
1	Director Applied Physics Laboratory The Johns Hopkins University Johns Hopkins Road Laurel, MD 20810
1	Massachusetts Institute of Technology Dept of Aeronautics and Astronautics ATTN: Tech Lib 77 Massachusetts Avenue Cambridge, MA 02139
1	Ohio State University Dept of Aeronautics and Astronautical Engineering ATTN: Tech Lib Columbus, OH 43210
2	Polytechnic Institute of New York Graduate Center ATTN: Tech Lib Dr. G. Moretti Route 110 Farmingdale, NY 11735
1	Director Forrestal Research Center Princeton University Princeton, NJ 08540

No. of Copies	Organization
1	Southwest Research Institute ATTN: Mr. Peter S. Westine P. O. Drawer 28510 8500 Culebra Road San Antonio, TX 78228

Aberdeen Proving Ground

Dir, USAMSAA
ATTN: DRXSY-D
DRXSY-MP, H. Cohen

Cdr, USATECOM
ATTN: DRSTE-TO-F

Dir, USACSL, Bldg. E3516
ATTN: DRDAR-CLB-PA